Communication

Dielectric Image Line-Based Leaky-Wave Antenna for Wide Range of Beam Scanning Through Broadside

Chandra Shekhar Prasad and Animesh Biswas

***Abstract*— In this communication, a dielectric image line (DIL)-based leaky-wave antenna is proposed with planar feeding. The dominant mode of DIL is perturbed by making holes periodically in the DIL and fast-wave space harmonics are generated. The proposed antenna is designed for Ku-band (12–18 GHz) and its impedance bandwidth in the fast-wave region is 36% (11.8–17 GHz). The scan range of the proposed antenna in the working band is 90° (−65° to 25°) and the gain is varying from 10 to 16 dBi in the fast-wave region. The proposed antenna can be directly scaled to other frequency bands by taking into account the corresponding dispersion characteristic in respective frequency bands. This scaling property is demonstrated in *V*-band. A prototype is fabricated and measured in Ku-band, which fairly agrees with simulated results.**

***Index Terms*— Broadband antennas, dielectric image line (DIL), frequency beam scanning, leaky-wave antenna (LWA), wide scan range.**

I. Introduction

To fulfill the demand of modern high rate and speed communications, imaging and radar systems, we need broadband, high gain, low profile, lightweight and easily integratable to other planar technology antennas. These goals can be achieved using leaky-wave antennas (LWAs) as these are traveling wave antenna (non-resonating), and hence, provide broad impedance bandwidth along with high gain (narrow beam). These antennas can be flush mounted and exhibit frequency and dielectric beam scanning properties [1].

Dielectric image line (DIL) can be a suitable candidate for higher frequency range as it has lower loss as compared to the other planar technology. The above mentioned goals can be easily achieved if we manage to design LWAs based on DIL which are simple and easy to fabricate and compatible to other planar technology.

An LWA can be made using periodically perturbing the DIL. In [2], dielectric grating periodicity is implemented in the inverted-strip dielectric waveguide to design an LWA and a band-reject filter in Ku-band. The reported antenna is scanning in the backward region. In this design, two different dielectric materials are used, one for guiding channel and another one for gratings. Grating dielectric slabs are pasted on the guiding channels which may not be suitable in millimeter-wave region. The mathematical formulation of periodic dielectric waveguide is presented in [3]. A dielectric grating antenna is proposed for millimeter-wave application in [4] and its theoretical insight is presented. Here, the basic structure is grounded dielectric slab waveguide and dielectric gratings are of the same material. The periodic dielectric loadings are used to get fast-wave space harmonics which are responsible for radiation. Here, stopband phenomena is observed in broad side direction. A circular dielectric rod grating antenna is proposed for millimeter-wave (Ka-band) application in [5].

Manuscript received December 26, 2016; revised May 11, 2017; accepted June 1, 2017. Date of publication June 9, 2017; date of current version August 2, 2017. *(Corresponding author: Chandra Shekhar Prasad.)*

The authors are with the Electrical Engineering Department, Indian Institute of Technology Kanpur, Kanpur 208016, India (e-mail: csprasad@iitk.ac.in; abiswas@iitk.ac.in).

Color versions of one or more of the figures in this communication are available online at http://ieeexplore.ieee.org.

Digital Object Identifier 10.1109/TAP.2017.2714024

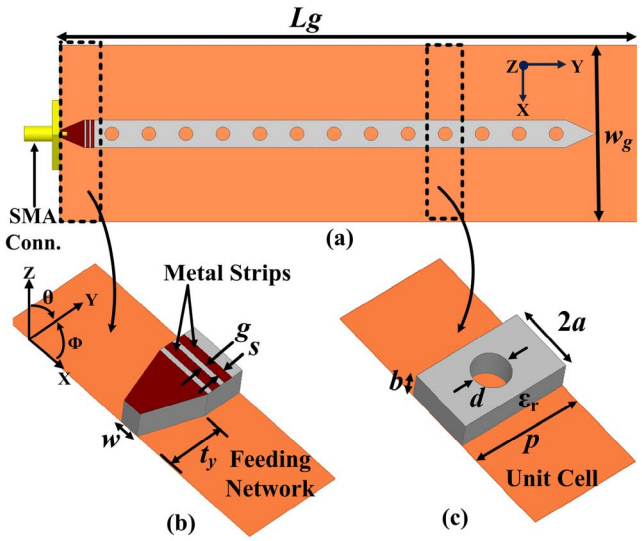

Fig. 1. Schematic of (a) full proposed antenna (b) feeding network and (c) unit cell. $L_g = 175$ mm, $w_g = 80$ mm, $2a = 6.25$ mm, $b = 2.54$ mm, $p = 10.75$ mm, $d = 3.5$ mm, $w = 2.54$ mm, $t_y = 5$ mm, $g = 0.3$ mm, $s = 0.6$ mm, and $\varepsilon r = 10.2$.

In [6], the performance of different dielectric gratings (like, isosceles trapezoid, right-angled triangle, isosceles triangle, and rectangular) a top of a wide grounded dielectric waveguide is studied and a rectangular dielectric grating-based antenna is proposed in Ka-band. A supercell dielectric grating (two layers of grating with different dimensions) is used for dual-beam LWA performance at 60 GHz in [7]. The dual beam is obtained using two space harmonics $n = -1$ and $n = -2$ and radiates in backward and forward region, respectively.

In all of the above mentioned LWAs, the dielectric gratings are placed on the top of the basic guiding structure. These gratings have same or different dielectric constant with respect to the basic guiding structure. In [8], an LWA based on rectangular dielectric gratings on the two sides of the DIL on a single substrate is proposed in *W*-band.

The DIL is also used as a feeder to achieve frequency beam scanned radiation pattern in dielectric resonators (DRs) array antennas. In [9], DR antenna array is proposed which is fed by slots in the ground plane of DIL. In this design, the DRs are pasted on the slots in the ground plane and the DIL is covered with metallic reflector to suppress the radiation by DIL itself. In [10], a DRs array antenna is proposed for *X*-band, in which DRs are placed according to Dolph– Chebyshev distribution on the same and one side of DIL. The DRs are excited by power coupling of DIL. In [11], a dielectric insular image line (DIIL)-fed DRs array antenna is proposed in Ka-band. The RDs are placed according to Taylor-distribution symmetrically on both left and right sides of the DIIL.

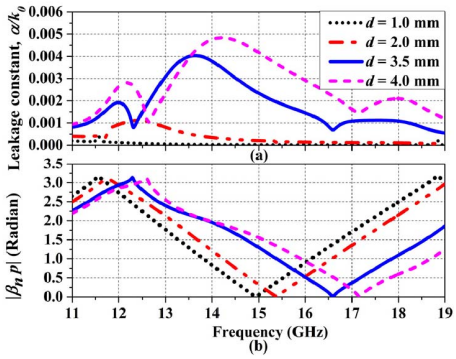

Fig. 2. Variation of (a) leakage constant and (b) propagation constant with the hole diameter.

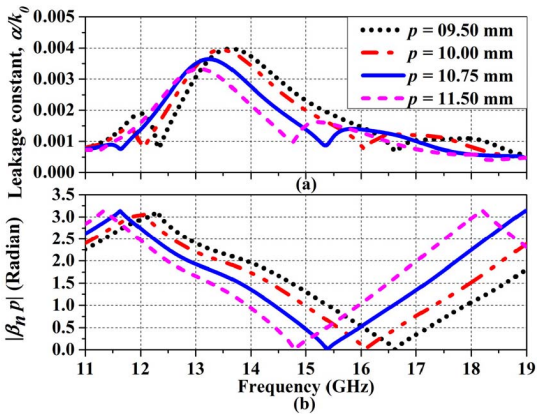

Fig. 3. Variation of (a) leakage constant and (b) propagation constant with the period of perturbation.

An LWA based on inset dielectric waveguide in frequency range of 50–85 GHz is proposed in [12]. A double-layered periodic-slotted ridged substrate integrated waveguide (SIW)-based antenna scanning through broadside is proposed in [13]. In [14], an LWA scanning through broadside, based on SIW technology, is presented.

In this communication, our focus is to develop an LWA for wide scan range without dielectric gratings using DIL which is without stopband, frequency scalable, and easy to fabricate. Section II is devoted for feeding network and antenna design approach. In Section III, the frequency scalability is presented with example and the measured results are presented in Section IV. Finally, conclusions are drawn in Section V.

II. Antenna Design Procedure

A. Design of Basic Dielectric Image Line

The basic structure of the proposed antenna with feeding network, which is used in simulation, is shown in Fig. 1, along with coordinate system. In Fig. 1, $2a$ is the width, b is the thickness of the DIL, p is the period of perturbation, d is the diameter of the hole. w and t_y are the width and tapered length of substrate truncated microstrip line, respectively, at the input. g and s are the gap and width of the metal strips, respectively, ε_r is the relative permittivity of the substrate, L_g and w_g are the length and width of the ground plane, respectively.

To use the DIL as the basic guiding structure for the LWA, it is necessary to design proper DIL for the particular frequency band of interest. We have three basic parameters for DIL design, namely, substrate (ε_r), thickness (b) and width ($2a$) of the substrate as shown in Fig. 1. The selection of the substrate is done in such a manner to minimize the radiation loss by DIL itself. To keep the radiation loss minimum by DIL itself, the selected substrate should have relatively high dielectric constant, so that fields are intact to the DIL. In this design, Rogers RT/duroid6010LM (tm) ($\varepsilon_r = 10.2$ and $\tan\delta = 0.0023$) is used.

After selecting the substrate, we are left to select the thickness and width of the DIL. Due to unavailability of all substrate thickness commercially, first we chose the suitable DIL thickness and then width accordingly. The field confinement and whether the DIL is working in single mode or multimode is determined by a/λ_0, where λ_0 is the free space wavelength at the design frequency. For unity aspect ratio ($b = a$), single-mode operation and good field confinement, it is calculated as [1]

$$\frac{b}{\lambda_0} \approx \frac{0.32}{\sqrt{\varepsilon_r - 1}}. \tag{1}$$

The calculated value of b using (1) at center frequency of Ku-band (15 GHz) is 2.11 mm. The nearest commercially available thickness 2.54 mm is taken in our design and the width ($2a = 5.08$ mm) is taken accordingly and optimized whenever needed.

B. Generation of Leaky Wave

For leaky wave generation, fast waves are required [15]. In the present structure, fast-wave spatial harmonics are generated using periodic perturbation of cylindrical holes along the axial line of basic structure. The cylindrical holes are drilled through the thickness of DIL which is very easy from fabrication point of view, unlike dielectric gratings on the top. According to Bloch–Floquet theory, periodic structure supports infinite number of space harmonics given by [15]

$$\beta_n(\omega) = \beta_0(\omega) + \frac{2n\pi}{p} \tag{2}$$

where $\beta_n(\omega)$ and $\beta_0(\omega)$ are the nth and fundamental space harmonics, respectively, p is the period and n is an integer. Generally, the fundamental space harmonic is slow wave but the space harmonic $n = -1$ is fast and it radiates in free space. The direction of radiation of the main beam in the periodic LWA for $n = -1$ space harmonics is calculated as [16]

$$\theta \approx \sin^{-1}\left(\frac{\beta_0(\omega)}{k_0} - \frac{2\pi}{k_0 \times p}\right) \tag{3}$$

where θ is the angle measured from Z-axis (Fig. 1) and k_0 is the free-space wavenumber at frequency of interest. Using (3), we can have the initial guess of period p for a particular main beam direction and frequency.

We are aiming to have main beam radiation at broadside ($\theta = 0°$) at 15 GHz. The calculated value of β_0/k_0 using Ansoft HFSS simulation is 2.1 at 15 GHz for $b = 2.54$ mm, $2a = 5.08$ mm, and $\varepsilon_r = 10.2$. The corresponding value of p is 9.52 mm and this is the initial value of period of perturbation which can be optimized for better performance.

C. Analysis of Unit Cell

The unit cell of the proposed antenna is shown in Fig. 1(c) with different parameters. The effective leakage (α) and propagation constant of the unit cell are calculated using the following [17]:

$$\beta_n p = \left|\mathrm{Im}\left(\cosh^{-1}\left(\frac{1 - S_{11}S_{22} + S_{21}S_{12}}{2S_{21}}\right)\right)\right| \tag{4}$$

$$\alpha p = \left|\mathrm{Re}\left(\cosh^{-1}\left(\frac{1 - S_{11}S_{22} + S_{21}S_{12}}{2S_{21}}\right)\right)\right|. \tag{5}$$

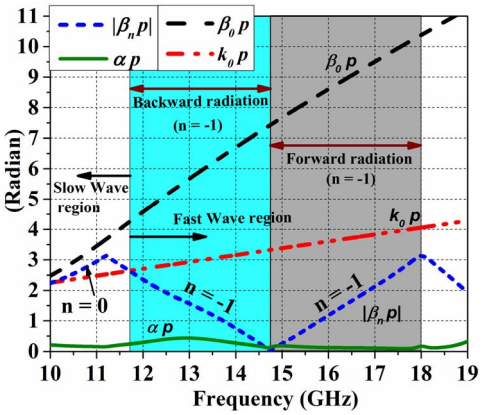

Fig. 4. Dispersion diagram of the final optimized unit cell.

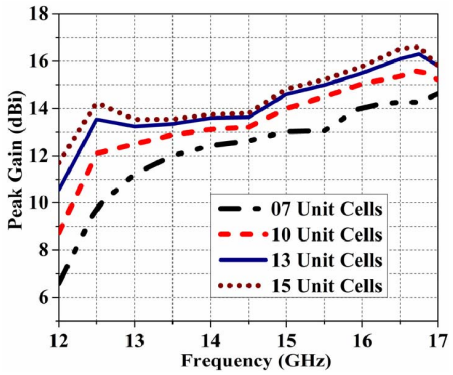

Fig. 5. Variation of peak gain with number of unit cells.

The S-parameters are extracted from the simulation of unit cell in HFSS. To calculate the leakage constant due to only radiation loss, perfect electric conductor, and lossless substrate are taken in simulation.

The selection of the diameter of the cylindrical perturbation is done on the basis of parametric studies. The variation of effective leakage and propagation constant with d is shown in Fig. 2. Fig. 2 depicts that the leakage constant is increasing and the broadside radiation ($\beta_n p = 0$) point is shifting to upper frequency from 15 GHz. For $d = 1$ mm, the radiation will be at broadside but the leakage rate is very low. To have sufficient radiation efficiency and limitation of available fabrication facility, $d = 3.5$ mm is taken in our design, although the broadside radiation is at 16.5 GHz, in this case.

Now, after fixing the value of d, we have only two variables, p and a, to optimize and achieve our goal. The main beam angle depends on β_0 and p mainly as per (2). The variation in β_0 is not much with a. Hence, p is optimized for broadside radiation around 15 GHz. The variation in leakage and propagation constant with p is shown in Fig. 3. The observation of Fig. 3(b) shows that the broadside radiation point is shifting toward 15 GHz for increasing value of p. In our final design, $p = 10.75$ mm is taken.

The value of parameter $2a$ is optimized in the final design of full structure including feeding network transition. In this antenna, a planar feeding network as discussed in [18] is used, whose basic configuration is shown in Fig. 1(b). The two metal strips used in the feeding structure basically to improve the impedance matching. In this design, we have taken $2a = 6.25$ mm for better matching.

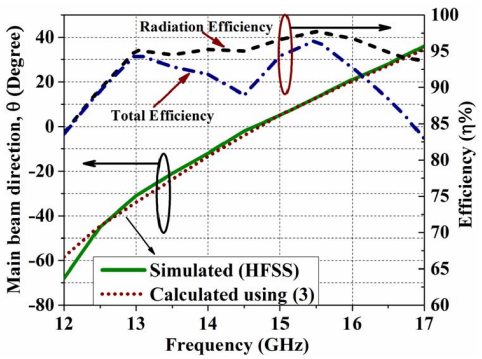

Fig. 6. Variation of main beam direction and radiation efficiency for 13 unit cell antenna with frequency.

D. Dispersion Diagram of Optimized Unit Cell

The dispersion diagram of the unit cell for the optimized data is depicted in Fig. 4. Fig. 4 shows that the fast-wave ($\beta_n p < k_0 p$) region starts from 11.8 GHz, so we expect the leaky-wave radiation from this frequency. The backward and forward radiation is also depicted in Fig. 4 for $n = -1$ space harmonic. The backward radiation takes place from 11.8 to 14.75 GHz and propagation constant drops to zero at 14.75 GHz which corresponds to broadside ($\theta = 0°$) radiation. After this point, forward region radiation is starting and going up to 18 GHz and after this $n = -2$ space harmonic starts.

E. Antenna Length Optimization

The gain of the traveling wave antenna depends on the length of the antenna. The variation of peak gain with number of unit cells is depicted in Fig. 5. From Fig. 5, we see that the peak gain variation is more from 7 to 13 unit cells and after that it is saturating. In our final fabrication, 13 unit cells are taken. The gain variation for this is around 6.3 dB (10–16.3 dBi). For reducing gain variation in the working frequency range, the antenna can be designed for a larger bandwidth than the actual working frequency range so that the unwanted gain variation in nonoperating band may be ignored.

The scan angle range, radiation efficiency, and total efficiency of the final antenna having 13 unit cells are depicted in Fig. 6. From Fig. 6, it is clearly visible that the simulated main beam scan range is around 95° (from −65° to 30°) from backward to forward region. It is also seen that the simulated beam angle is well matching with calculated one. The simulated radiation efficiency of the proposed antenna is better than 90% above 12.5 GHz.

III. Scaling in V-Band

In this section, the frequency scaling property of the Ku-band antenna is presented. The optimized antenna at 15 GHz is scaled to 60 GHz by dividing the antenna parameters $2a$, b, p, and d by four. The feeding network section parameters like w, t_y, g, and s are calculated accordingly, using the methods in [18]. In this, instead of SMA, standard V-connector is used in simulation to make it reliable for measurement. The S-parameter response of this scaled antenna without any optimization along with its dimensions are shown in Fig. 7. From Fig. 7, we see that the $|S_{11}|$ is below −10 dB up to 65.5 GHz. The simulated radiation pattern of the scaled antenna from 51 to 65.5 GHz is shown in Fig. 8. From Fig. 8, we see that the main beam is scanning with frequency from backward to forward region. The scanning range is around 66° (from −41° to 25°) and the maximum gain is 15.3 dBi at 63 GHz for 13 unit cell antenna. It is to be notice that the scan angle range is not same as that of the

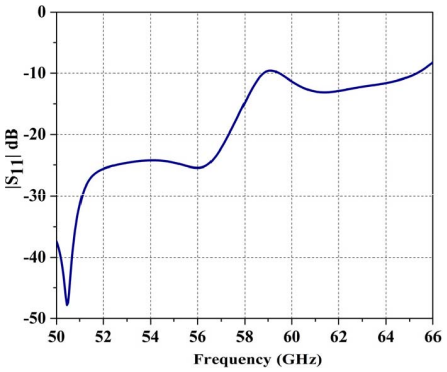

Fig. 7. S-parameter response of V-band antenna. Here, $L_g = 43.75$ mm, $w_g = 20$ mm, $2a = 1.5625$ mm, $b = 0.635$ mm, $p = 2.6875$ mm, $d = 0.875$ mm, $w = 0.635$ mm, $t_y = 0.9$ mm, $g = 0.09$ mm, $s = 0.18$ mm, and $\varepsilon_r = 10.2$.

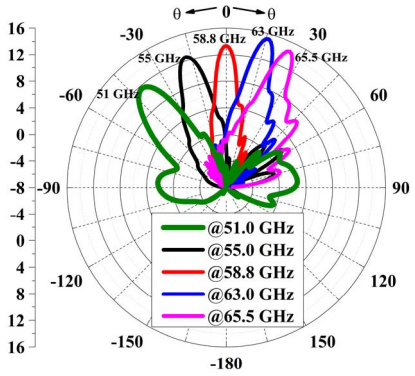

Fig. 8. E-plane radiation pattern of V-band antenna.

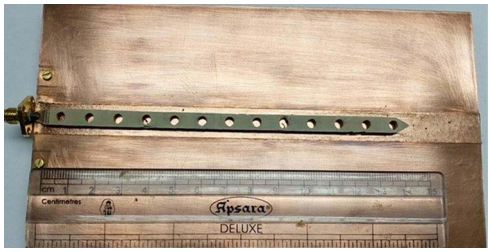

Fig. 9. Fabricated prototype of Ku-band design.

Ku-band design. This is mainly due to the fact that the β_0/k_0 curve slope is not same in both the bands. The main beam is directed to broadside at 58.8 GHz, which is exactly four times of the Ku-band antenna broadside radiation frequency. The S-parameter response, gain, and scan angle range can be improved by optimizing the antenna parameters.

IV. Measurements

To validate the design, a prototype at Ku-band is fabricated and measured. The fabricated prototype is shown in Fig. 9. The cutting and drilling of the substrate are done by abrasive water jet and chemical etching is used to remove the metal coating. At the end of the antenna, substrate is tapered to avoid any reflection back to the input. After cutting and etching, the structure is pasted on the copper ground plane using double-sided adhesive copper tape. The measured and simulated S-parameter and gain responses are depicted in Fig. 10. From Fig. 10, we observe that the S-parameter and gain

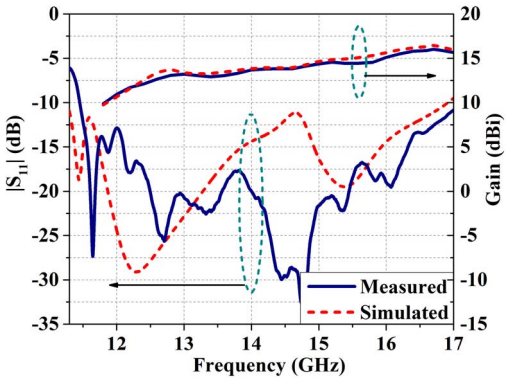

Fig. 10. Measured and simulated S-parameter and gain responses.

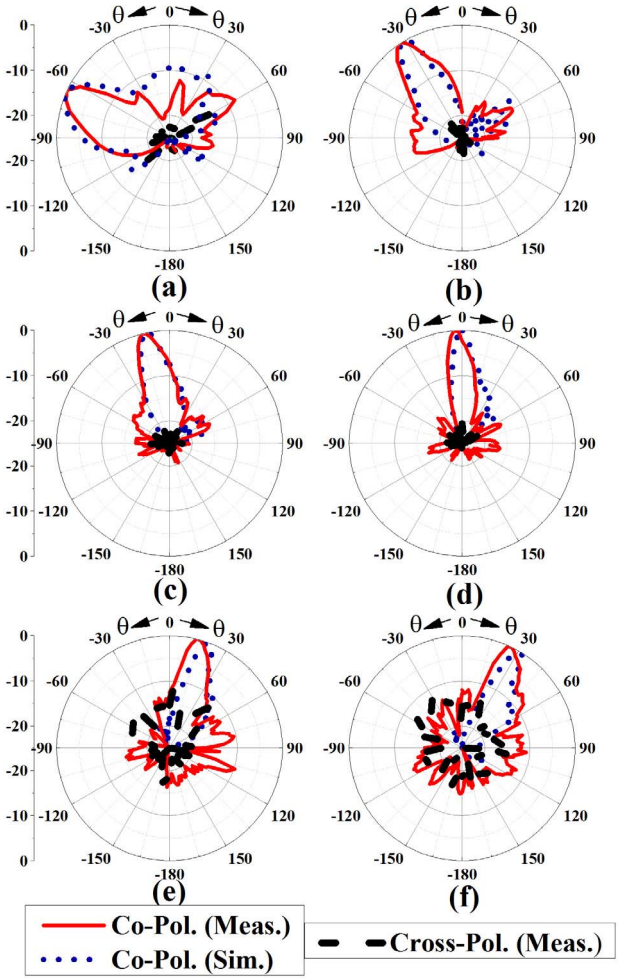

Fig. 11. Measured and simulated E-plane radiation patterns at (a) 12 GHz, (b) 13 GHz, (c) 14 GHz, (d) 14.8 GHz, (e) 16 GHz, and (f) 16.8 GHz.

response are fairly agree with simulated one. The peak gain in the fast-wave region is varying between 10 and 16 dBi and the $|S_{11}|$ is below -10 dB in the same range.

The proposed antenna is able to radiate fan beam (XZ-plane) with continuous beam scanning in YZ-plane. The measured and simulated 2-D E-plane radiations are depicted in Fig. 11. From Fig. 11, we see that the measured and simulated copolarization patterns are matching well except some variation at upper frequency. The simulated range of scanning of main beam is 95° ($-65°$ to 30°) and the corresponding

TABLE I

PROPOSED ANTENNA PERFORMANCE COMPARISON

	[7]	[8]	[12]	[13]	[14]	**This Work**
Freq. (GHz)	57-63	97-103	50-85	8-12	9-14	**11.8-17**
L_{ant}	$58\lambda_0$ @60GHz	$5\lambda_0$ @100 GHz	$8\lambda_0$ @60 GHz	N.A	$6\lambda_0$ @ 12 GHz	**$7\lambda_0$ @ 15 GHz**
No. of beams	Dual (n=-1, n=-2)	Single (n=-1)	Single (n=-1)	Single (n=-1)	Single (n=-1)	**Single (n=-1)**
Radiation at $\theta = 0^0$	No	No	Yes	Yes	Yes	**Yes**
Scan range	22^0 to 30^0 -30^0 to -20^0	-20^0 to -2^0	-9^0 to 40^0	-35^0 to 35^0	-40^0 to 35^0	**-65^0 to 25^0**
Gain (dBi)	20 to 25, 20.5 to 23.5	18 @ 100 GHz	9.1 to 14.2	10.5 to 12.5	8 to 13	**10 to 16**

measured range is 90° (−65° to 25°) for the frequency range of 12–16.8 GHz. It is to be noted that the backward and forward beam scanning are not symmetrical. The forward scan range can be improved maintaining the backward beam position if we can manage to improve the impedance matching up to 18 GHz (single-beam fast-wave region). The measured cross-polarization levels are better than 20 dB in the main beam direction at all frequencies in the operating range as shown in Fig. 11. The simulated cross-polarization level is below 30 dB at all frequencies and not shown here. The deviation of measured response from the simulated one, may be due to fabrication, dielectric tolerance, etc.

The performance of the proposed antenna is compared with other relevant antennas available in literature and is shown in Table I.

V. CONCLUSION

In this communication, we have introduced a new periodic LWA based on the DIL technology. In this design, instead of a top or side dielectric grating, holes are used in DIL, which make it easy to fabricate and compact. The designed antenna exhibits broad impedance bandwidth (36%) in the fast-wave region, wide range (90°) of continuous beam scanning though broadside. It has also the capability of direct frequency translation to other frequency band. The scan range is dependent on the dispersion characteristic in that band. The frequency scaling property is validated by an example in *V*-band.

REFERENCES

[1] P. Bhartia and I. J. Bahl, *Millimeter Wave Engineering and Applications*. New York, NY, USA: Wiley, 1984.

[2] T. Itoh, "Application of gratings in a dielectric waveguide for leaky-wave antennas and band-reject filters (short papers)," *IEEE Trans. Microw. Theory Techn.*, vol. 25, no. 12, pp. 1134–1138, Dec. 1977.

[3] S. T. Peng, T. Tamir, and H. L. Bertoni, "Theory of periodic dielect waveguides," *IEEE Trans. Microw. Theory Techn.*, vol. 23, no. 1, pp. 123–133, Jan. 1975.

[4] F. K. Schwering and S.-T. Peng, "Design of dielectric grating antennas for millimeter-wave applications," *IEEE Trans. Microw. Theory Techn.*, vol. 31, no. 2, pp. 199–209, Feb. 1983.

[5] S. Xu, J. Min, S.-T. Peng, and F. K. Schwering, "A millimeter-wave omnidirectional circular dielectric rod grating antenna," *IEEE Trans. Antennas Propag.*, vol. 39, no. 7, pp. 883–891, Jul. 1991.

[6] H. F. Hammad, Y. M. M. Antar, A. P. Freundorfer, and M. Sayer, "A new dielectric grating antenna at millimeter wave frequency," *IEEE Trans. Antennas Propag.*, vol. 52, no. 1, pp. 36–44, Jan. 2004.

[7] Z. L. Ma, K. B. Ng, C. H. Chan, and L. J. Jiang, "A novel supercell-based dielectric grating dual-beam leaky-wave antenna for 60-GHz applications," *IEEE Trans. Antennas Propag.*, vol. 64, no. 12, pp. 5521–5526, Dec. 2016.

[8] A. Zandieh, A. S. Abdellatif, A. Taeb, and S. Safavi-Naeini, "Low-cost and high-efficiency antenna for millimeter-wave frequency-scanning applications," *IEEE Antennas Wireless Propag. Lett.*, vol. 12, pp. 116–119, 2013.

[9] A. S. Al-Zoubi, A. A. Kishk, and A. W. Glisson, "Aperture coupled rectangular dielectric resonator antenna array fed by dielectric image guide," *IEEE Trans. Antennas Propag.*, vol. 57, no. 8, pp. 2252–2259, Aug. 2009.

[10] A. S. Al-Zoubi, A. A. Kishk, and A. W. Glisson, "A linear rectangular dielectric resonator antenna array fed by dielectric image guide with low cross polarization," *IEEE Trans. Antennas Propag.*, vol. 58, no. 3, pp. 697–705, Mar. 2010.

[11] L. Jin, R. Lee, and I. Robertson, "A dielectric resonator antenna array using dielectric insular image guide," *IEEE Trans. Antennas Propag.*, vol. 63, no. 2, pp. 859–862, Feb. 2015.

[12] X. Bai, S. W. Qu, K. B. Ng, and C. H. Chan, "Sinusoidally modulated leaky-wave antenna for millimeter-wave application," *IEEE Trans. Antennas Propag.*, vol. 64, no. 3, pp. 849–855, Mar. 2016.

[13] A. Mallahzadeh and S. Mohammad-Ali-Nezhad, "Periodic collinear-slotted leaky wave antenna with open stopband elimination," *IEEE Trans. Antennas Propag.*, vol. 63, no. 12, pp. 5512–5521, Dec. 2015.

[14] Y. L. Lyu *et al.*, "Leaky-wave antennas based on noncutoff substrate integrated waveguide supporting beam scanning from backward to forward," *IEEE Trans. Antennas Propag.*, vol. 64, no. 6, pp. 2155–2164, Jun. 2016.

[15] A. Hessel, *Antenna Theory, Part II*, R. E. Collin and R. F. Zucker, Eds. New York, NY, USA: McGraw-Hill, 1969, ch. 19.

[16] J. L. Volakis, *Antenna Engineering Handbook*, 4th ed. New York, NY, USA: McGraw-Hill, 2007.

[17] D. M. Pozar, *Microwave Engineering*, 2nd ed. New York, NY, USA: Wiley, 1998.

[18] C. S. Prasad and A. Biswas, "Broadband planar transition to dielectric image line by substrate truncated microstrip line for millimeter-wave circuit integration," *IEEE Microw. Wireless Compon. Lett.*, vol. 27, no. 6, pp. 533–535, Jun. 2017.